Pediatric Cardiology
https://doi.org/10.1007/s00246-024-03441-9

RESEARCH

Differential Regulation of Immune-Related Genes in the Developing Heart

Mathieu Garand[1] · Susie S. Y. Huang[1] · Brian Dineen[1] · Ian A. Glass[2] · Pirooz Eghtesady[1]

Received: 21 November 2023 / Accepted: 2 February 2024

Abstract

In many congenital heart defects, it can be difficult to ascertain primary pathology from secondary consequences from altered flow through the developing heart. The molecular differences between the growing right and left ventricles (RV and LV, respectively) following the completion of septation and the impact of sex on these mechanisms have not been investigated. We analyzed RNA-seq data derived from twelve RV and LVs, one with Hypoplastic Left Heart Syndrome (HLHS), to compare the transcriptomic landscape between the ventricles during development. Differential gene expression analysis revealed a large proportion of genes unique to either the RV or LV as well as sex bias. Our GO enrichment and network analysis strategy highlighted the differential role of immune functions between the RV and LV in the developing heart. Comparatively, RNA-seq analysis of data from C57Bl6/J mice hearts collected at E14 resulted in the enrichment of similar processes related to T cells and leukocyte migration and activation. Differential gene expression analysis of an HLHS case highlighted significant downregulation of chromatin organization pathways and upregulation of genes involved in muscle organ development. This analysis also identified previously unreported upregulation of genes involved in IL-17 production pathways. In conclusion, differences exist between the gene expression profiles of RV versus LV with the expression of immune-related genes being significantly different between these two chambers. The pathogenesis of HLHS may involve alterations in the expression of chromatin and muscle gene organization as well as upregulation of the IL-17 response pathway.

Keywords Developmental biology of the heart · Congenital heart disease · Birth defect · Right ventricle · Left ventricle · Cardiac chambers · Hypoplastic left heart syndrome · Interleukin-17 · Helper T cells

Introduction

Nearly 1% of infants worldwide are born with a congenital heart defect (CHD) [1]. The causes for more than half of CHDs are unknown [2], but it is believed that alterations in active developmental pathways during the first 8 weeks of life account for the majority. Most research on heart development has been focused on this rather early period. Little is known about how factors beyond this period may contribute to the progression of cardiac defects.

Cardiac defects are often present as either "left-sided" or "right-sided", where pathology predominantly affects a single chamber. In many of these instances, it can be difficult to ascertain primary pathology from secondary consequences from altered flow through developing heart. For instance, Hypoplastic Left Heart Syndrome (HLHS), a very severe CHD requiring multiple palliative surgeries followed by a heart transplant during a child's life [3, 4], involves a spectrum of malformations characterized by the underdevelopment of

✉ Pirooz Eghtesady
eghtesady670@wustl.edu

Mathieu Garand
garand@wustl.edu

Susie S. Y. Huang
susie.sy.huang@gmail.com

Brian Dineen
b.dineen@wustl.edu

Ian A. Glass
ianglass@uw.edu

[1] Division of Pediatric Cardiothoracic Surgery, Department of Surgery, Washington University School of Medicine, St. Louis, MO, USA

[2] Department of Pediatrics and Medicine, University of Washington, Seattle, WA, USA

Published online: 13 March 2024

left-sided structures including the left ventricle (LV) [5]. In some babies, HLHS is fully manifest by 12 weeks of gestation. In other instances, HLHS evolves during fetal life from primary aortic stenosis [6, 7]. Conversely, in Tetralogy of Fallot, a defect characterized by "right-sided" pathology, an anteriorly malaligned conal septum can result in significant hypertrophy of the right ventricle (RV) and is associated with RV outflow tract abnormalities such as pulmonary valve or branch pulmonary artery stenoses [8]. In both conditions, the typical pattern of intracardiac blood flow is disrupted, potentially exacerbating abnormalities in development. These reflect the importance of understanding the baseline molecular differences between the developing RV and LV for greater insight into the pathogenesis of CHD.

Prior studies have shown differential oxygen exposure and cardiac output between the fetal RV and LV [9, 10], which could also result in modulation of varied metabolic pathways or responses to oxygen content for each chamber [11–14]. Additionally, sex can interact significantly with the prevalence and severity of CHDs [15, 16]. For example, HLHS is significantly associated with Turner Syndrome, with a slight predominance in males [17–19]. Little is known about possible differences in these attributes in the developing RV versus LV and how they may contribute to the development or the progression of CHDs. These unique in utero physiologic milieus and possible inherent differences between RV and LV development could play a part in both the natural and un-natural (i.e., CHD) development of the ventricles. Hence, understanding potential differences in the molecular pathways functioning in each ventricle during development could lead to better understanding of observed CHD pathology.

In this study, we performed mRNA-seq analysis to gain insight into ventricle-specific gene expression changes during gestation. Our study included 11 unaffected hearts and one heart with HLHS. We interpreted ventricle-specific transcriptome differences using multivariate, gene ontology over-representation, network enrichment, and systematic literature mining. In the process, we found notable differences in the expression of immune-related genes between the RV and LV which revolved around the '*positive regulation of CD4 T cells*', '*upregulation of IFN γ production and signaling pathway*', and '*positive regulation of TH17 differentiation and response*' (representative GO terms italicized). Finally, we examined putative molecular contributors to the pathogenesis of HLHS in an index case.

Material and Methods

mRNA-Sequencing

Total RNA samples were provided by the University of Washington Birth Defects Research Lab (BDRL, IRB STUDY00000380) and prepared for Illumina HiSeq 2500 Sequencing using the SMARTer Ultra Low RNA kit (Takara-Clontech) according to manufacturer's protocol. Sequencing was performed using single-end reads (50 bases) and at a read depth of 30 M per sample. Basecalls and demultiplexing were performed with Illumina's bcl2fastq software and a custom python demultiplexing program with a maximum of one mismatch in the indexing read. mRNA-seq reads were aligned to GRCh38 (GENCODE 20) with STAR version 2.0.4b. Fetal mouse heart mRNA-seq data (C57Bl6/J; E14; $n = 5$, contributing 3 RV and 2 LV) were obtained from a previous study [20]. A count per million threshold equivalent to ~10 raw expression value was applied to remove all lowly expressed genes and only genes above the threshold and having ≥ 5 samples were kept. Due to the small sample size, no outliers (> 1.5 SD from the means) were removed from the human dataset and no outliers were identified for the mouse dataset. Filtered transcripts were then annotated to gene symbols using org.Hs.eg.db and org.Mm.eg.db. A table of individual subject characteristics can be found in the online resources (Online Resource 10).

Differential Gene Expression Analysis

The *DEseq2* package was used to determine differentially expressed genes (DEGs) between two groups. When necessary, *FDRtool* was utilized to correct over-estimation of the assumed null distribution variance by Wald Test, which is indicated by a hill–shaped p-value histogram. In brief, the z-scores returned by *DEseq2* was used as input to *FDRtool* to re-estimate the p-values that were then adjusted for multiple comparisons by the Benjamini–Hochberg method. Genes were considered differentially expressed if they had a $|\log_2 FC| > 2$ for human or $|\log_2 FC| > 1.5$ for the mouse dataset and a padj < 0.05 for all contrasts. To evaluate the immune components of the DEGs identified, we retrieved comprehensive lists of immune-related genes in humans from *InnateDB* [21], *ImmPort,* and *IRIS* databases. A list of 6231 genes was used to identify the immune-related genes in this study.

Gene Ontology (GO) Enrichment Analysis

The list of DEGs was submitted, as a single-gene set per comparison, to query for GO terms associated with biological processes via the gene over-representation test (*enrichGO*), against the background gene set, using the package *ClusterProfiler*. The minimal gene set size of three and an FDR < 0.05 cutoff was set to determine significance. The enriched GO terms were then reduced for term redundancy using the function *simplify()*, with *dispensability cutoff = 0.7*. We then functionally re-clustered select lists of DEGs to refine the over-representation GO enrichment test as described by Huang et al. [22]. In brief, the semantic

similarity of the DEGs were calculated using the *GoSemSim* package [23] with the Wang method. The correlation matrix was obtained with *method = "spearman"* and *hclust method = "complete"*. Clusters were then determined using *dynamicTreeCut* package [24], with a minimum gene size set at 30 and 15 for the human and mice dataset, respectively, *method = "hybrid"*, and *deepSplit = 0*. The functional clusters of DEGs were then re-submitted for GO enrichment analysis using "*compareCluster()*" with the aforementioned parameters and the enriched GO terms reduced for semantic redundancy. Visual summary of representative subset of terms was performed with *Revigo* [25].

Network Enrichment Analysis

A list of 278 DEGs unique to the unaffected right vs left ventricle comparison were further subjected to network analysis with GO Biological Processes and GO Immune System Process databases and *ClueGO* were used to determine and visualize the enrichment networks. The following parameters were used to construct the enrichment network: min/max GO level = 4–8, Number of Genes = 3, Min Percentage = 4, Kappa Score Threshold = 0.45, Sharing Group Percentage = 50 and the statistical significance was set at Benjamini–Hochberg adjusted p-value < 0.05.

Literature Mining—Acumenta Literature Lab (LitLabTM)

LitLab™ (Acumenta Biotech, USA) allows the identification of biological and biochemical terms that are significantly associated with the literature from a gene set. The analysis provides additional meaning to experimentally derived gene and protein data [26]. The LitLab™ database contains current gene, biological, and biochemical references in every indexed PubMed abstract and are updated quarterly (> 35 million abstracts, as of January 2023). LitLab™ calculates the frequencies of the input genes with > 86,000 terms in the Literature Lab™ database (as of December 2022) and compares the values with that of a 1000 random gene sets, containing the same number of genes and literature volume profile as the experimental set, to determine statistical significance (cutoff at p-value < 0.0228). LitLab™ is composed of four main applications: Term Viewer, PLUS, Editor, and Gene Retriever.

Results

Characteristics of the Overall Transcriptomic Profiling

Among the 12 examined RNA samples, eight were female (one with HLHS with likely aortic stenosis and mitral stenosis variety based on gross examination) and four were male. The average gestational age was at 88 days or 12 weeks + 4 days (range 78 to 98 days or 11 weeks + 1 to 14 weeks). On average, 27 M read depth was achieved, with the alignment rate of uniquely mapped reads averaging at 65%, a median mapped read of 12 M, and the median number of transcripts detected at 15,712 (Online Resource 1a–b). The relatively low alignment rate is expected for a single-end short fragment library (50 bp) and is deemed appropriate for gene expression analysis [27]. The count density distributions were found to be homogeneous and peaked at $8\log_2$ counts per million among the samples (Online Resource 1c). A total of 14,586 genes remained after gene-level filtering and conversion to gene symbols using *org.Hs.eg.db*. Annotation to gene biotype revealed predominately protein-coding genes (89%) (Online Resource 1d). The normalized expressions of the select housekeeping genes (GAPDH, GUSB, IPO8, POLR2A, and YWHAZ) [28] were not significantly different between the left and right ventricles (Online Resource 2a). Principal component analysis of the overall gene expression indicated that the inter-individual difference contributed to 29% of the variance (PC1) and partly trended with gestational age (Online Resource 2b). Taking the top 1000 highly variable genes among the ventricles highlighted a clear separation by sex across PC2 (13%) (Online Resource 2c–d). Thus, we considered sex as a potential confounder and performed downstream analyses while segregating by sex.

Differentially Expressed Genes Identified Between RV and LV

To explore the inherent gene expression differences between the developing ventricles, we performed differential gene expression analysis, excluding the single HLHS case, between the following groups: 1) All RV vs LV ($n = 11$ vs 11), 2) Female RV vs Female LV ($n = 7$ vs 7) and 3) Males RV vs Males LV ($n = 4$ vs 4). We defined the significant DEGs as those with an absolute $\log_2$ fold change (FC) > 2 and a padj < 0.05 (full list provided as Online Resource 11). We observed a total of 529 (332 up- and 197 down-regulated), 563 (300 up- and 263 down-regulated), and 219 (140 up- and 79 down-regulated) DEGs

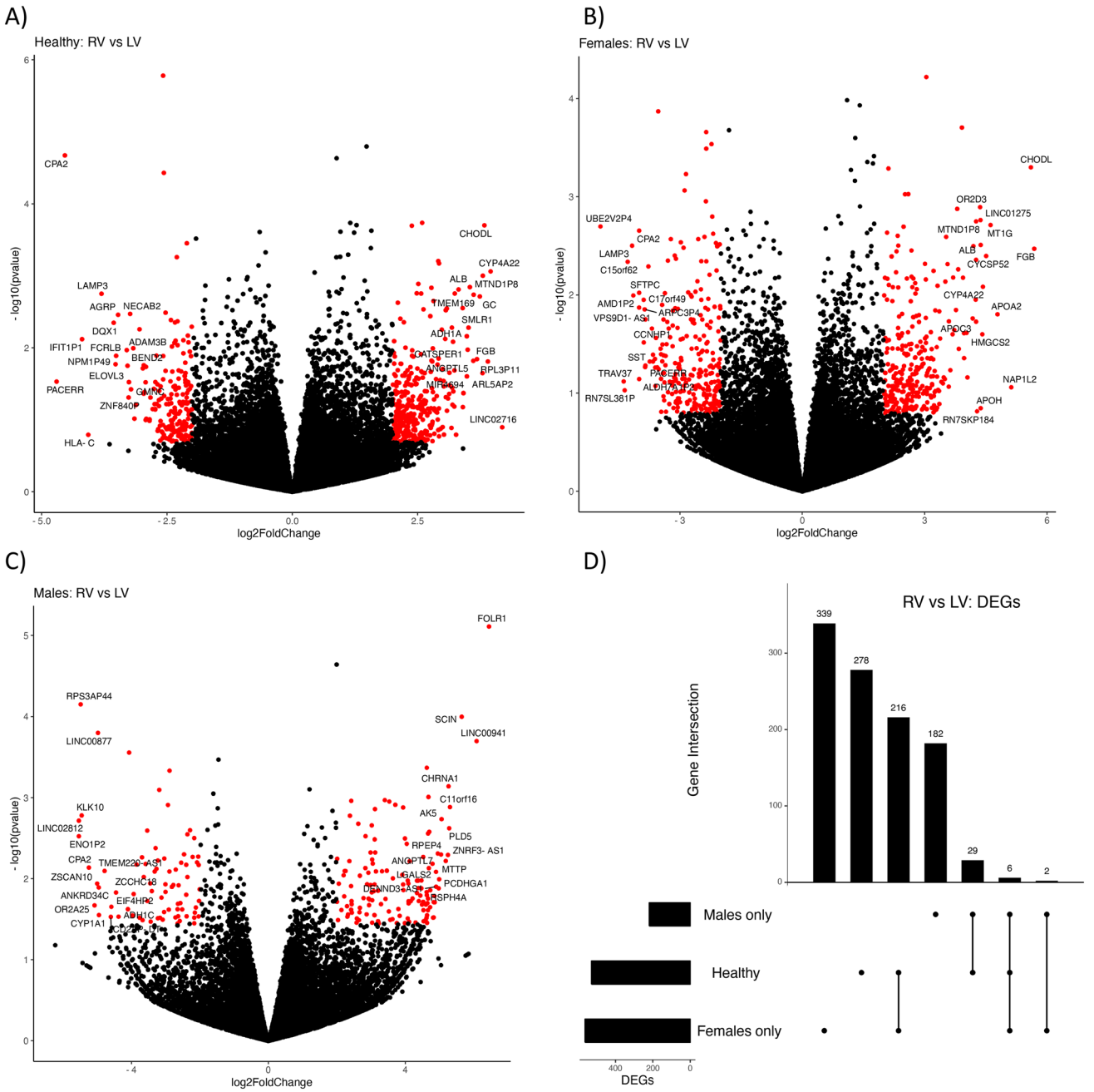

Fig. 1 Significant DEGs between the right and left ventricles exhibit a high proportion of uniqueness. Differential gene expression analysis comparing ventricle sides. (**a**) among healthy (i.e., unaffected) hearts, (**b**) within female subject only, and (**c**) within male subjects only. (**d**) Summary and intersection of DEGs identified among all comparisons as indicated. Each gene is represented by a dot. Significance of the DEGs, red dots, were defined by the following thresholds: |log2FC|> 2 and p.adjust < 0.05

in the aforementioned group comparisons, respectively (Fig. 1 a–c). Differences in sample size likely account for the lower number of DEGs identified when looking only at males. Of note, sex determination was further confirmed by assessing the expression of sex biomarkers XIST, TSIX (female) and DDX3Y (male) [29] as well as differentially expressed markers CD99 (higher in males) [30] and KDM6A (higher in females) [31] (data not shown). Majority of the DEGs were unique to the three different comparisons, as shown by the intersection analysis (Fig. 1d, Online Resource 12). The effect of sex was examined within each of the ventricle types and returned relatively small lists of DEGs for RV (43; 30 up- and 13 down-regulated) and LV (31; 19 up- and 12 down-regulated) when comparing

Males vs Females (n = 4 vs 7) (Online Resource 12). Overall, we did not observe differential expression of genes involved in cardiac asymmetry or chamber/arch development (sources: Reactome R-HSA-1181150, MSigDB M10039, and [32–39]) (data not shown).

Biological Modulations Inherent to the Ventricles Clearly Implicated Differential Immune Functions

GO Enrichment Analysis Using the Lists of DEGs Directly as Inputs

To gain knowledge of the biological processes ascribed to the differentially expressed genes, we performed GO enrichment analyses via the over-representation test and using individual lists of DEGs as inputs. The analysis returned 34 significantly enriched GO terms for the All RV vs LV group and 4 terms, relating to hydrolase and peptidase activities, for the Female RV vs Female LV comparison (Online Resource 13). There were no GO term enrichments returned for any of the other comparisons, namely: Males, RV vs LV; RV, Males vs Females; and LV, Males vs Females. The lack of GO enrichment suggests that not enough related DEGs were identified to enrich a particular biological/molecular pathway. Additionally, for the Males vs Females comparisons, some of the DEGs are known sexually dimorphic genes (e.g., XIST, TIST, DDX3Y) where their differential expression is driven by chromosome bias [40]. However, we can't rule out the effect of the reduced group size of the comparisons (7 Females vs 4 Males) for obtaining a small number of DEGs and the lack of GO term enrichment.

Prior Functional Re-Clustering of the Lists of DEGs Improved GO Enrichment Results

To improve the sensitivity and coverage of the enriched biological processes, we subclustered the lists of DEGs on the basis of the semantic similarity of their associated GO terms prior to re-analysis. We increased the enriched GO terms to four and eightfold for the All RV vs LV and Female RV vs LV comparisons, respectively (Fig. 2a–b). In addition, eight terms were found enriched for the Males RV vs LV comparison, which previously had no significant enrichments (Fig. 2c). For the All RV vs LV comparison, the GO terms can be clustered into three board categories: (1) regulation of hemostasis, retinol and triglyceride metabolism, and HDL remodeling, (2) T cell-mediated immunity, and cellular stress response and detoxification of metal ion, and (3) negative regulation of neurogenesis, positive regulation of JAK-STAT pathway, pituitary gland development, and positive regulation of hormone metabolic process. Regulation and metabolism of small biomolecules including vitamins, lipids, and hormones, stood out as the predominant processes among sex-specific groups, i.e., the processes were enriched in sex-specific RV vs LV comparisons but not seen in the top GO enriched from all sex combined RV vs LV. (Fig. 2b–c). Since the enrichment of biological processes is dependent on the input DEGs list, it is expected to see more granularity with the larger contrast, All RV vs LV ($n = 22$), which recapitulate findings from both female and male only comparisons. Interestingly, 'retinol metabolic process' was persistently enriched across all comparisons (female, male, or altogether) and was primarily driven by the differential expression of cytochrome P450 complex proteins and an infant-specific metabolic enzyme (ADH1A). To help summarize the categories of GO terms, we reduced and visualized the enriched terms obtained from the All RV vs LV comparison using *Revigo* [25] (Fig. 2d). With this approach, it was easier to appreciate additional subsets of enriched GO terms; the representative term for each subset is indicated in the plot (see Online Resource 13 for full lists).

Network Mapping of GO Terms and DEGs Highlight a Putative Role for the Th1 and Th17 Pathways

The significant enrichment of immune-related genes between the RV and LV was further investigated by performing the enrichment analysis with only the DEGs uniquely identified when comparing All RV vs LV (278 genes); illustrated in Online Resource 5a. GO enrichment analysis returned 28 GO terms (Online Resource 5b). This comparison provided enhanced granularity about the putative immune processes involved, such as interferon gamma signaling pathway, Th17cell-mediated immunity, interleukin-17 production, and T cell activation and cytotoxicity. This result suggests that the differential expression of genes relating to immune processes between RV and LV are not influenced by sex. To gain insights into processes specifically influenced by sex, we conducted an enrichment analysis on DEGs exclusively identified when comparing RV vs LV in females (399 genes) and males (182 genes) separately (Online Resource 6a). Among females, the distinctive genes enriched 9 GO terms related to 'negative regulation of peptidase' and 'RAS protein signal transduction,' neither are known to exhibit sex-specific functions (Online Resource 6b). Conversely, in males, the unique genes did not yield enrichment for any GO terms. Using a network approach, we mapped the interactions between GO terms and DEGs and found an intricate cluster of T cell-related function (Fig. 3). In our analysis, IFNg takes a central role in the network and, along with IL12R and TBX21 (which encodes the transcription factor T-bet), promotes the positive regulation of CD4 T cells and Th1 differentiation; PRKCQ can contribute to Th1 bias by inducing IL-2 and T-bet expression [41, 42]. Regulation of Th17 immune response is also

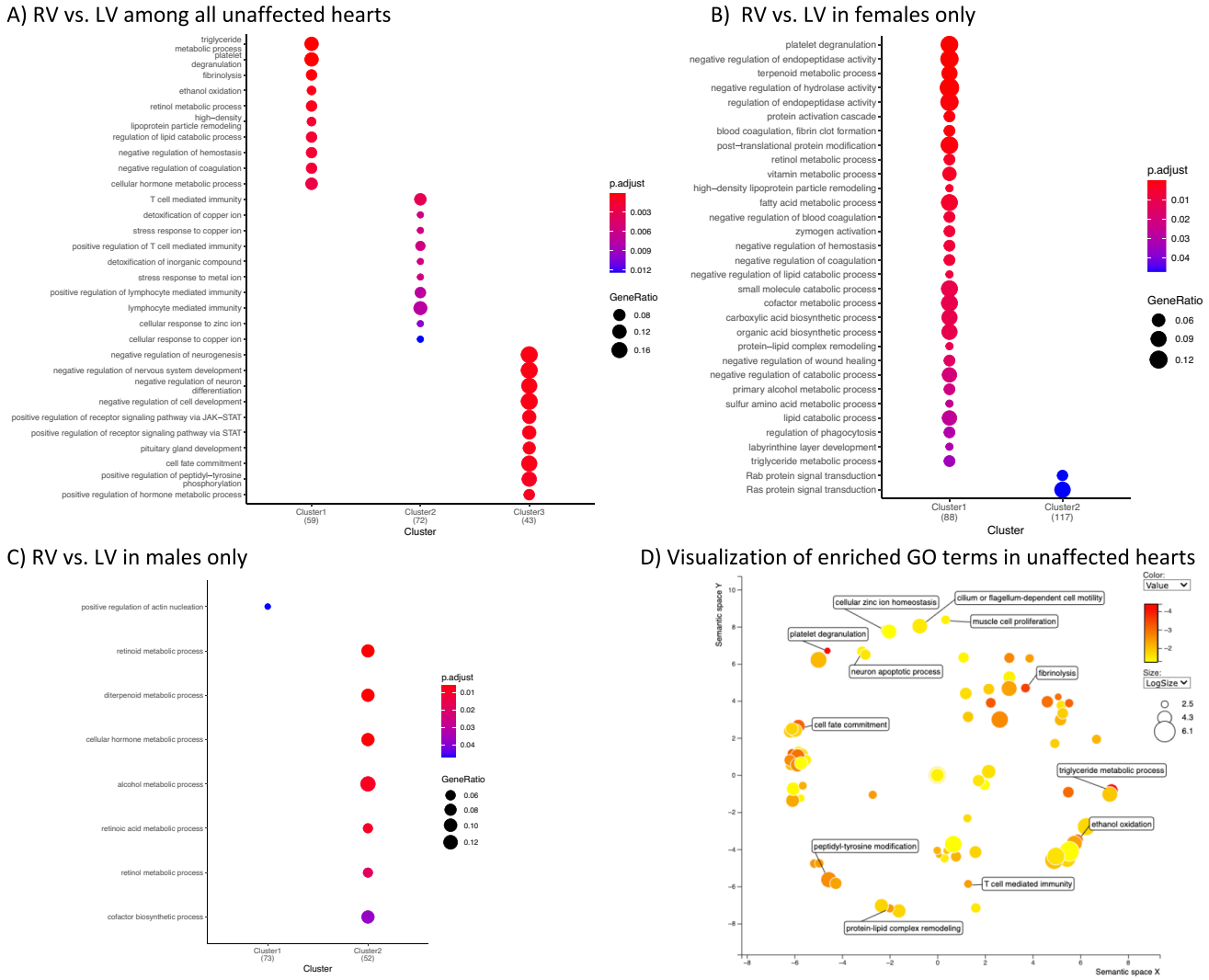

Fig. 2 Semantic similarity clustering of the DEGs' function prior to GO enrichment analysis increased sensitivity and coverage by four to eightfold. The diagrams summarize the GO terms enriched, separated into clusters based on semantic similarity of the biological processes, and with the number of DEGs that contribute to the GO enrichment indicated in parentheses. (**a**) The RV vs LV comparison among all the unaffected hearts revealed three major clusters, (**b**) RV vs LV comparison among females returned two clusters, and (**c**) RV vs LV comparison among males returned two clusters with markedly less enriched terms. (**d**) Visual summary of representative subsets of terms enriched when comparing RV vs LV DEGs in unaffected hearts using a term similarity-based clustering. REVIGO determines subset 'Representative' terms by prioritizing the terms with higher 'uniqueness' while also considering enrichment p-values to guide the selection

prominent with PRKCQ having a known role in Th17 differentiation [42] and IL-17 production [43]; PKC-theta leads to activation of SRC1 which then interacts with RORgT and induces IL-17A production [44]. OSM signals through its receptor and activates STAT family proteins. Interaction with OSM type 1 receptor, especially, induces STAT3 expression which has been shown essential for Th17 differentiation [45]. Collectively, these findings imply that Th1 and Th17 pathways play a differential role in the developing ventricles.

Comparison with Mouse Model Data

Mammalian models such as mouse are by far the most practical means to study fetal development both for ethical and technical reasons. However, molecular and mechanistic studies in mice have rarely been directly compared to humans [46], especially when comparing ventricle-specific gene regulation. We re-analyzed mRNA-seq data from of C57Bl6/J mice collected at embryonic age E14 that was generated from a previous study [20] and are

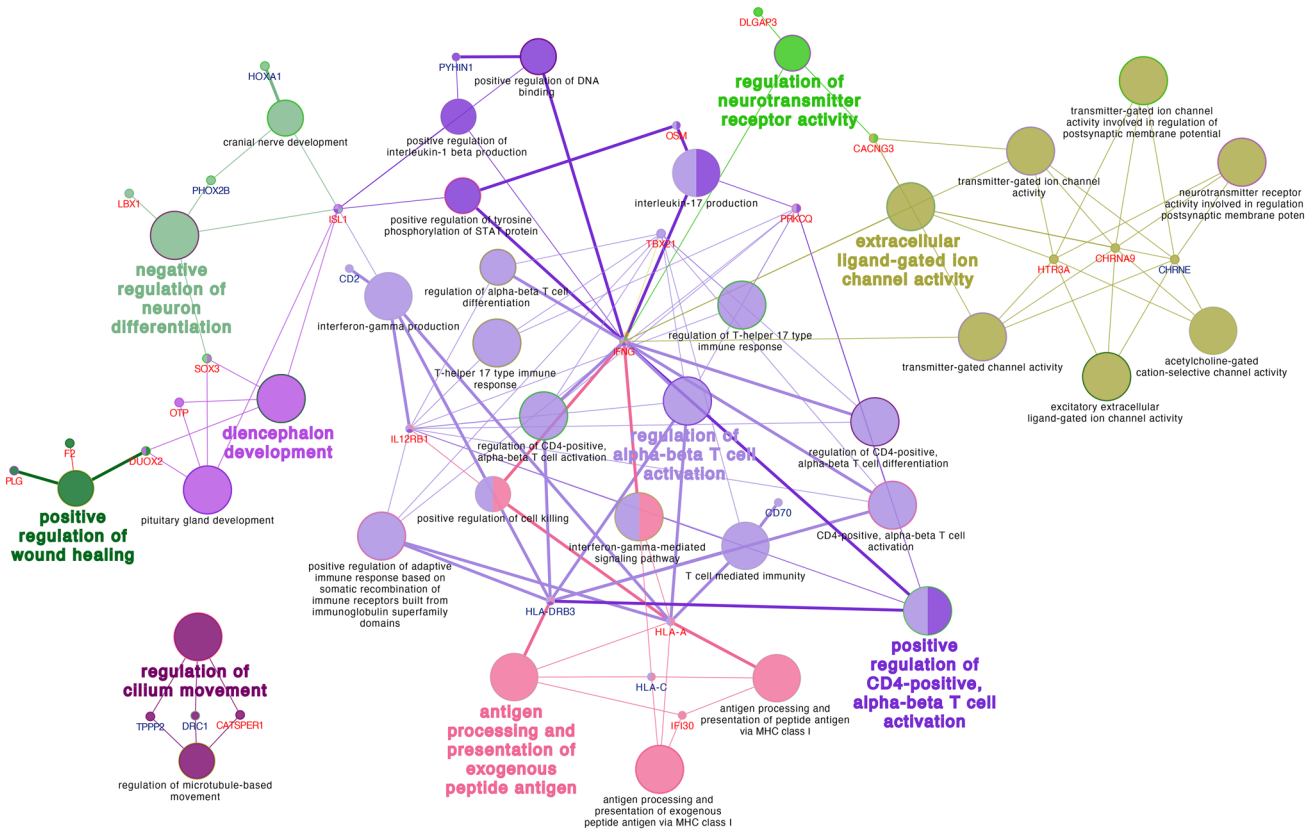

Fig. 3 GO and DEGs interaction network emphasizes the differential role of immune functions between the RV and LV of the developing heart. The node color indicates biologically similar reactions and the size reflects the number of genes contributing to the pathway. If the reaction pathway shares 50% or more of the contributing genes, then they are connected by an edge. The representative nodes (based on statistical significance) are indicated by the colored texts. Genes are denoted by small dots with color matching the GO terms to which they belong. The font color for the gene represents up– (red) or down– (blue) regulation

available at NCIBI GEO under dataset ID GSE157522. The total number of genes expressed that remained after filtering and gene symbol annotation was 12,813; among which 93% were found to be protein-coding. Normalized expressions of Gapdh, Ppia, and Pgk1, robust housekeeping genes for mouse fetal heart, were not significantly different between the two ventricles. We found 82 DEGs ($|\log2FC| > 1.5$ and $padj < 0.05$) between the RV and LV in our mouse dataset (Online Resource 7a, Online Resource 11). The resulting enrichment of GO terms highlighted processes such as cell adhesion and leukocytes and T cells migration/proliferation (Online Resource 7b). We observed a lack of granularity among the GO terms which can in part be due to the small sample size, yielding a smaller number of informative DEGs. Key differences compared with the biological process enrichment obtained in the human samples were hydrogen peroxide metabolism, gas transport, and regulation of muscle fiber development.

HLHS

Repression of Epigenetic/DNA Organization and Upregulation of Muscle Development in HLHS

To examine the differential gene expression in the heart with HLHS, we used RV and LV as independent samples and compared the HLHS heart to the equivalent aggregate of unaffected hearts. Thus, 147 (51 up– and 96 down–regulated) DEGs were obtained comparing HLHS ($n = 2$) vs. unaffected hearts ($n = 22$) (Online Resource 8a, Online Resource 11). The DEGs enriched 30 GO terms (Online Resource 8b) which increased to 35 after functionally clustering the DEGs (Fig. 4a). The GO enrichment showed major downregulation of genes relating to epigenetic regulation of gene expression, chromatin organization, protein-DNA complex organization, and DNA conformation change. As well, major upregulation of genes involved in muscle organ development, contraction, and response to mechanical

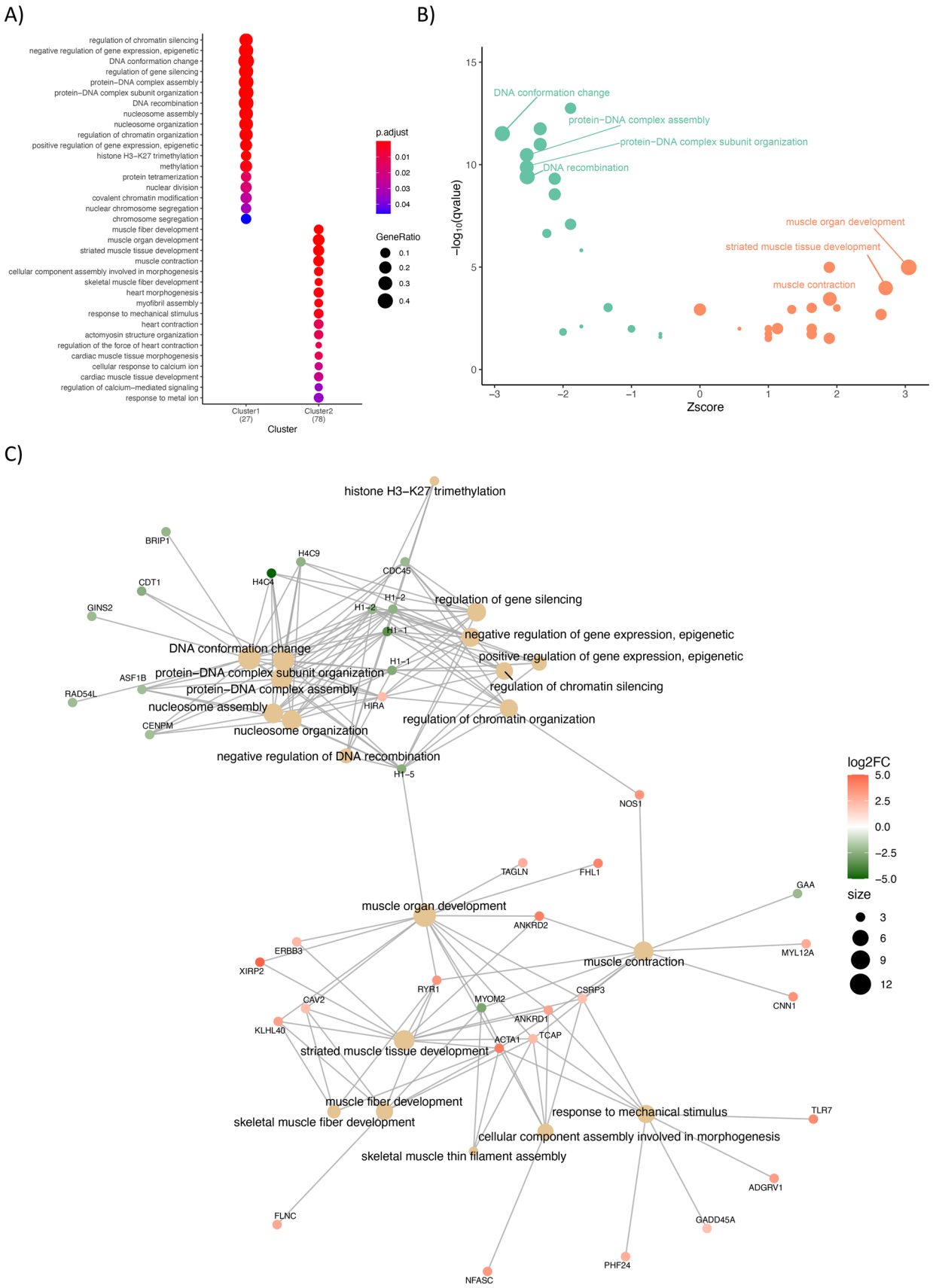
A)
regulation of chromatin silencing
negative regulation of gene expression, epigenetic
DNA conformation change
regulation of gene silencing
protein−DNA complex assembly
protein−DNA complex subunit organization
DNA recombination
nucleosome assembly
nucleosome organization
regulation of chromatin organization
positive regulation of gene expression, epigenetic
histone H3−K27 trimethylation
methylation
protein tetramerization
nuclear division
covalent chromatin modification
nuclear chromosome segregation
chromosome segregation
muscle fiber development
muscle organ development
striated muscle tissue development
muscle contraction
cellular component assembly involved in morphogenesis
skeletal muscle fiber development
heart morphogenesis
myofibril assembly
response to mechanical stimulus
heart contraction
actomyosin structure organization
regulation of the force of heart contraction
cardiac muscle tissue morphogenesis
cellular response to calcium ion
cardiac muscle tissue development
regulation of calcium−mediated signaling
response to metal ion
Cluster1 (27)
Cluster2 (78)
Cluster
p.adjust
0.01
0.02
0.03
0.04
GeneRatio
0.1
0.2
0.3
0.4
B)
DNA conformation change
protein−DNA complex assembly
protein−DNA complex subunit organization
DNA recombination
muscle organ development
striated muscle tissue development
muscle contraction
−log10(qvalue)
Zscore
C)
histone H3−K27 trimethylation
BRIP1
H4C9
CDC45
CDT1
H4C4
H1−2
regulation of gene silencing
GINS2
negative regulation of gene expression, epigenetic
DNA conformation change
positive regulation of gene expression, epigenetic
protein−DNA complex subunit organization
ASF1B
regulation of chromatin silencing
protein−DNA complex assembly
RAD54L
nucleosome assembly
HIRA
regulation of chromatin organization
CENPM
nucleosome organization
negative regulation of DNA recombination
H1−5
NOS1
TAGLN
FHL1
GAA
muscle organ development
ANKRD2
ERBB3
MYL12A
XIRP2
muscle contraction
RYR1
CSRP3
CAV2
MYOM2
CNN1
ANKRD1
KLHL40
TCAP
ACTA1
striated muscle tissue development
muscle fiber development
response to mechanical stimulus
TLR7
skeletal muscle fiber development
cellular component assembly involved in morphogenesis
skeletal muscle thin filament assembly
ADGRV1
FLNC
GADD45A
PHF24
NFASC
log2FC
5.0
2.5
0.0
−2.5
−5.0
size
3
6
9
12

◂**Fig. 4** Major molecular changes in the HLHS case pertain to DNA organization and muscle development compared with that of the combined healthy left and right ventricles. (**a**) The diagram summarizes the GO terms enriched, separated into clusters based on semantic similarity of the biological processes, and with the number of DEGs that contribute to the GO enrichment indicated in parentheses. (**b**) Enriched GO terms are plotted based on their $-\log_{10}$(qvalue) and Zscore. This score was calculated from the sums of up– and down–regulated DEGs divided by the square root of the total number of genes which contributed to the enrichment of the term. (**c**) The network shows the GO terms enriched as yellow nodes and the genes contributing to the enrichment, linked by edges, are depicted by small dot colored based on their $\log_2$FC

stimulus (Fig. 4b). We generated a network of the genes, along with their $\log_2$FC, and GO terms (Fig. 4c), to provide further insights on the key factors that drive the differences in the biological process. Several histone genes (e.g., H1-1, H1-2, H1-5 H4C4, H4C9) and replication regulators (e.g., CDC45, H3K27me3, CDT1, GINS2, ASF1B) were significantly downregulated. On the other hand, some genes related with muscle development have relatively unknown mechanisms (e.g., FHL1, XIRP2), and yet have several diseases associations. Other genes (ACTA1, ANKRD2, ANKRD1, RYR1) support upregulation of muscle formation. An increased prevalence of HLHS has been documented in males and females with Turner syndrome. To determine this possibility, we manually curated gene biomarkers of Turner syndrome in female from the literature [47, 48] and compared the gene expression in the HLHS case vs all the other hearts. We found no significant differences, suggesting Turner's syndrome was likely not in play in our index case of HLHS.

DEGs–Literature Associations Highlight PAI-1 Upregulation in HLHS

To gain further perspective about the biological and biochemical processes associated with our list of 147 DEGs, we utilized two literature mining solutions, LitLab™ and Gene Retriever™ (Fig. 5). This approach identified Medical Subject Headings (MeSH) terms significantly associated with our DEG list, providing information derived from peer-reviewed publications. Seven clusters of terms were identified, including dilated cardiomyopathy, hypertrophic cardiomyopathy, cardiac calcium regulation, plasminogen activator inhibitor-1 (PAI-1), beta-catenin, and WNT signaling pathways. The involvement of antifibrinolytic pathways provided an interesting novel avenue to explore. In the literature, PAI-1 deficiency in 12 to 20 weeks old mice has been associated with upregulation of TGFb expression from cardiomyocytes and contribute to the development of cardiac fibrosis [49, 50]. In 12-week-old mice, expression of PAI-1 has been shown to provide a protective effect to cardiac stress response in a model of cardiac hypertrophy and fibrosis [51]. In our data, SERPINE1, the gene that encodes for PAI-1, is significantly upregulated by 15-fold in the RV of the HLHS case compared with the unaffected (data not shown). This surprising observation could represent a compensatory mechanism.

IL-3 and IL-36, Downstream Targets of IL-17A, are Significantly Upregulated in HLHS

To contrast immune gene expression in our data, we interrogated the ImmPort database [52] which is a curated list of 4677 immunologically relevant genes. We identified four genes and pseudogenes each that were significantly upregulated in HLHS compared with normal hearts: IL3, TRAV16, IL36B, CD300LD, IGLV8OR8-1, FKBP1AP3, CEACAMP2, GLYATL1P4. The expression of those 8 genes is mostly absent in unaffected heart while they are elevated (between 4 and 16-fold) in our HLHS heart. A seeded-network analysis approach was used to infer interacting protein and deduced enrichment in the IL-3 signaling pathway, autophagy/aggrephagy, and tyrosine phosphorylation. IL36 and IL3 are induced by IL-17A and positive synergistic and negative regulatory effects, respectively [53, 54]. The TRAV16 gene codes for a V region of the variable domain of T cell receptor alpha chain [55]. The CD300 family is composed of membrane receptor proteins that modulate a broad and diverse array of immune cell processes such as the positive regulation of IL-6 and TNFa production [56]. Recently, CD300LD was identified as a receptor of norovirus entry [57]. IGLV8OR8-1, CEACAMP2, GLYATL1P4 are pseudogenes. Also, FKBP1AP3 is a pseudogene of FKBP12, a major T cell immunoregulator of TGFb and ryanodine receptors (RYR) activity. Of note, RYR1 is significantly upregulated (10.8-fold) in HLHS compared with unaffected heart in our analysis.

TGFb, IL-17, and p53 Pathways Enriched by Differentially Expressed ISGs in HLHS

In a single-cell analysis of unaffected hearts, Suryawnshi et al. identified 18 cell types, including 6 types of immune cells. When contrasted to a heart with congenital heart block, the authors found that all cell types overexpressed interferon-stimulated genes (ISGs) and 'interferon signaling' was also identified as the most up-regulated biological process according to pathway analysis of the overall DEGs. In our data, contrasting ISGs (sources: MSigDB M15615 and M13453) expression between HLHS vs unaffected hearts revealed 14 differentially expressed genes ($p < 0.05$); TRIM26, CSRP3 (involved in myogenesis), PTPN11 (implicated in Noonan syndrome), RBBP4, CASP8, SF3A1, HADHB, BBC3 (regulate by p53, binds Bcl-2), SMAD4 (TGFb signaling), SRSF2, SKP1, FOSL1, CYCS

Fig. 5 Literature association analysis reinforces the GO term enrichment results comparing ventricles from unaffected vs HLHS hearts. We used Literature Lab (LitLab™) to perform an association analysis of the 147 DEGs between ventricles from HLHS and unaffected hearts with the current body of scientific literature. Briefly, LitLab™ queried the PubMed database (> 35 million abstracts, as of January 2023) for articles associated with the gene list of interest and returned the tagged Medical Subject Headings (MeSHs) with statistical significance. This analysis yielded seven MeSH terms clusters

(cytochrome C), DDX17. Interestingly, TGFb, IL-17, and apoptosis/p53 pathways were enriched by those 14 genes using PROGENy (data not shown), a bioinformatic approach that infer signaling activity of pathways from gene expression while taking into consideration post-translational modification [58].

Discussion

Over the last three decades, tremendous insights have been gained regarding early developmental changes in the embryonic heart, leading to the formation of the well-recognized four chambered structure [59, 60]. Much less, however, is known about the activities that occur over the ensuing time that prepares the heart for postnatal circulation. To our knowledge, our report is the first to systematically examine DEGs between the left and right ventricles. The interpretation of our results can be mapped to a time point where key developmental events (e.g., septation) have already completed. Nevertheless, in humans, the months that follows completion of cardiac morphogenesis can still allow cardiac defects to develop due to hemodynamic remodeling.

Our study reveals several notable findings that differentiate the developing RV and LV. First, sex was a factor affecting gene expression profiles, a novel finding that aligns

with the known differences in both propensity toward certain defects [15, 61] as well as manifestations of response to circulatory effects of CHD [62, 63]. Our finding also aligns at the molecular level with the study by Synnergren et al. where they compared RA vs LV in paired adult (58–80 years old) males and females and identified more protein-coding genes involved in immune function in females than in males (12). Second, our results showed major differential expression of immune genes between RV and LV, perhaps suggestive of differential activity of remodeling between the two ventricles during development. Thus far, there have been only a few investigations exploring the role of the immune system in cardiac development. Lastly, our examination of an unique case of HLHS highlights the potential role of histone modifiers and chromatin access as well as cardiomyocyte contractile activity. Additionally, our findings point to a dysregulation of the Th1/Th17 balance via upregulation of genes promoting IL-17 production in the HLHS case, perhaps reflective of a compensatory mechanism in response to other primary pathology within the developing LV. Given the constraint of having only one HLHS case, this aspect of our study is inherently exploratory, and as such, will require further validation with a larger cohort.

The development of the heart left–right asymmetry has been well studied across species during embryonic life. In vertebrates, asymmetry is caused by nodal cilia and coordinated differential expression of genes, especially transcription factors [35, 59, 64]. In the fetal heart, some pathways, such as the Nodal pathway, have been linked to asymmetry and cardiac defects [32, 34, 65]. Perhaps not surprisingly, in our dataset, genes belonging to the NODAL-signaling (source: R-HSA-1181150) and cardiac chamber/arch development pathways [66, 67] were not differentially expressed between ventricles except for a significantly lower TBX5 expression in RV than in LV (data not shown). This may reflect the lesser involvement of these genes during post-septation phase of development. TBX5 is a gene encoding a transcriptional activator involved in atrial natriuretic factor (ANF) gene regulation. In mice, at E11.5 (equivalent to 7 weeks + 1 to 7 weeks + 3 in human [46]), Tbx5 is expressed in the myocardium of RA, LA, AVC, and LV, while expression of both Tbx5 and ANF is virtually absent from the RV and outflow track [66]. In this regard, our findings aligned with prior reports, given our samples correspond to a later developmental stage (11 weeks + 1 to 14 weeks).

Oxygen content in the heart must be tightly regulated as hypoxia induces essential growth factors but a severe lack of oxygen causes irreversible damage [68]. Further, unique circulation leads to differential blood flow with different oxygen contents through the developing heart. Therefore, differential gene expression may affect development by modulating oxygen availability or responses to hypoxia. To explore the relationship between ventricles and oxygen-responsive pathway, we contrasted the HIF1a, VEGF, "response to oxygen species", and "response to oxygen levels" pathways (sources: hsa04066, hsa04370, GO:0000302, and MSigDB GO:0070482, respectively) between ventricles. In our data, there were no differences in the expression of genes involved in these pathways between ventricles.

Left to right asymmetric expression of immune genes has been demonstrated in adult hearts in animal models. Greater expression of immune genes has been reported in the RV of adult male rats compared with LV in both normoxic and hypoxic conditions [13]. Differential expression of immune genes between RV and LV has been shown in 8–10 weeks old mouse hearts exposed to cold ischemic conditions [14]. As part of the present study, we compared RV and LV from fetuses of mice at embryonic age E14 and found enrichment of cell–cell adhesion and leukocytes and T cells migration/proliferation in the RV. In humans, differential expression of immune-related gene has been reported between the RA and LV of the adult male hearts [12]. However, no studies have been performed looking at spatial differences of immune-related gene expression and how this may impact cardiac development.

In our study, when comparing RV vs LV from the unaffected hearts, IL-17 production was significantly upregulated in the RV. IL-17A is known to induce expression of IL-36 [69] and IL-3 [70]. Interestingly, we observed upregulation of IL-36 and IL-3 (8 and 12-fold) expression in the RV of our HLHS case than in its LV and to all the ventricles of the unaffected hearts (data not shown). IL-36 and IL-17A have been shown to synergistically induce inflammation with TNFα in human endothelial cells and keratinocytes [53, 69, 71]. On the other hand, IL-3 may act as a negative regulator of the Th17 pathway, preventing the development of autoimmune response [54] and has been shown to be essential for cardiac development in zebrafish [72]. Additionally, several genes promoting the Th17 differentiation pathway (source: hsa04659) – such as IL-23, IL-23R, IL-17F/A, IL-1b, and RORC – had markedly elevated expression in RV of our HLHS case compared with the other hearts (Online Resource 9). Notably, the expression of the RORC gene (coding for RORy/RORyT which is involved in upregulation of IL17A production [73]) and NCOA1 gene (encoding for SRC-1, a co-activator of RORy activity [74]) were six–eightfold higher in both ventricles of our HLHS case compared with the unaffected heart ventricles (data not shown). To summarize the findings regarding DEGs relevant to the Th1 and Th17 pathways, we constructed a network diagram highlighting the key genes significantly upregulated in the HLHS case compared to the healthy (Fig. 6). The source of IL-17 is another very interesting topic and could arise from a unique embryonically-derived subset of γδT17 cells [75], where RORyT, along with STAT3, are critical for gdT17 differentiation during the embryonic phase [76,

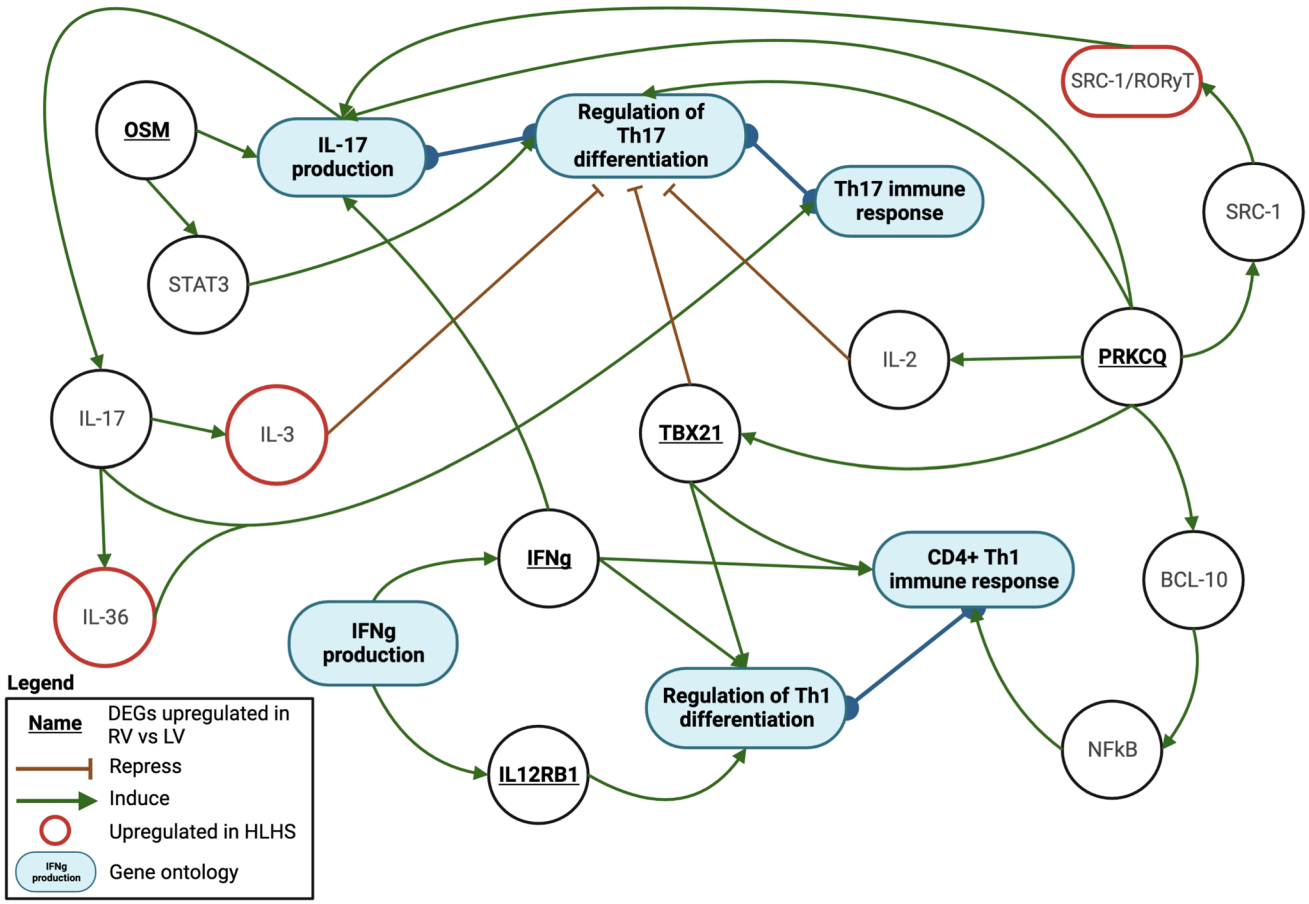

Fig. 6 Network diagram summarizing the differential regulation of the Th1 and Th17 pathways in the HLHS ventricles compared to all the unaffected ventricles. DEGs analysis between the RV and LV identified upregulation of several immune genes (indicated in bold and underlined text within circle). Based on the associations with GO terms and known functions reported in the literature, arrows indicating induction (green pointy arrows) and repression (brown blunt arrow) are depicted between the genes and GO terms. The expression of IL-3, IL-36, and SRC-1/RORγT genes were significantly upregulated in the HLHS case compared to the unaffected hearts and are highlighted by red circles. Significantly enriched GO terms are depicted by blue ovals with blue shading. Closely related GO terms have a connecting dark blue line between them

77]. In short, the increased expression of IL17 may either reflect a bystander effect (i.e., increased inflammation in the neighborhood leads to increased expression of IL-17) or a key contributor to evolving the pathology in HLHS.

Using an underdeveloped left ventricle and HLHS newborn-derived iPSC-endocardial cells, Miao et al. [78] showed that intrinsic endocardial defects and an abnormal endocardial population could contribute to the pathogenesis of HLHS. Potential indirect involvement of the immune system in cardiac development has been hinted in the past. Cui et al. carried out scRNA-seq of 18 human embryos, spanning 5 to 25 weeks gestational age [59]. Although focused on the whole-heart as opposed to RV versus LV, they identified three types of immune cells in the developing heart: mast cells, macrophages, and B/T cells. Previously, CCR2- macrophages were shown to remodel the coronary plexus by modulating blood vessel expansion and expression of growth factors [67, 79]. Additionally, endocardially derived tissue macrophages (EcTM) have been shown to be essential in the remodeling of aortic and mitral valves [80]. Comparing the enriched gene signature of EcTM in our data revealed elevated expression of CD44 (lymphocyte activation, recirculation, and homing; cell adhesion; cancer) and CD74 (antigen presentation MCHII) in the HLHS heart compared with the unaffected hearts. Cell surface CD74 serves as a receptor for macrophage migration inhibitory factor (MIF) on many cell types; MIF binding to CD74 induces a signaling cascade that results in regulation of cell proliferation and survival. These findings support a role for the immune system in HLHS, perhaps as part of local tissue remodeling [81].

Apart from the immune system, we also identified genes involved in retinol metabolism, metal ion detoxification, and neuronal differentiation between RV and LV

of the unaffected hearts. The rational for these differential enrichments is less clear. Atypical retinol metabolism has been linked to many developmental issues in mice [82–84] and is perhaps related to altered retinoic acid regulation of neural crest cell migration [85–89]. In our dataset, three metallothionein protein-coding genes (MT1G, MT1M, and MT1H), a family of cysteine-rich metal chelators which bind and decrease levels of free metal ions, were upregulated in the unaffected RV compared with LV. Metal ions have been implicated in the regulation of immune function, although the mechanisms remain largely unknown [90]. Alternatively, these differences may reflect the physiologic differences between the RV and LV in utero (e.g., the RV provides a higher cardiac output than the LV). Overall, from our results, we are unable to determine in what way retinol metabolism, metal ion detoxification, and neuronal differentiation are affecting functions in the ventricles, and these findings require further exploration.

The study has certain limitations that warrant consideration. The lack of sufficient clinical information prevents us from obtaining a detailed knowledge regarding the HLHS case (e.g., absence or presence of endocardial fibroelastosis or exact status of the mitral or aortic valve or other associated abnormal histologic abnormalities). Additionally, analytical constraints arise from the reliance on a single-case for comparison with an unaffected group. Inferences were made from combining ventricles of the HLHS case to allow statistical testing at the expense of losing ventricle-specific information. Despite the exploratory nature of this approach and limitations, the study revealed unique gene expression patterns associated with HLHS and underscores the need for further validation with a larger cohort. This approach aligns with other research leveraging single-case scenarios to generate hypotheses and advance understanding in heart development and pathology [91, 92].

Conclusion

Little is known about differential gene expression in the developing ventricles following septation and how alteration of the associated molecular pathways may contribute to the pathophysiology of CHDs. Our findings suggest a major part of the differently enriched signaling pathways between the right and left developing ventricles relates to immune function, previously not reported. Our analyses also bring novel evidence for possible implication of Th17 cells in HLHS in addition to genes related to chromatin organization and muscle contraction. The detailed ventricle-specific information in our data enriches the existing knowledge base, providing a foundation for deeper exploration into the intricacies of human heart development and disease pathogenesis.

Supplementary Information The online version contains supplementary material available at https://doi.org/10.1007/s00246-024-03441-9.

Author Contributions SSYH, MG, IAG, and PE conceptualized the study. IAG contributed to methodology and investigation. SSYH, MG, BD, and PE performed formal analysis. SSYH, MG and PE wrote the original draft. IAG and PE provided resource and funding. All authors have read and approved the final manuscript. Criteria are as indicated by the contributor roles taxonomy.

Funding Funding was provided by NIH under NICHD Grant # R24HD000836, to IAG. The study was supported by SLCH Research Foundation. PE is also supported by the Emerson Chair in Pediatric Cardiothoracic Surgery.

Data Availability Data publicly available on the NCBI GEO repository after publication of the article (ascension number: TBD).

Declarations

Conflict of interest The authors declare no competing interests.

Ethical Approval Not applicable.

Consent to Participate Not applicable.

References

1. van der Linde D, Konings EE, Slager MA et al (2011) Birth prevalence of congenital heart disease worldwide: a systematic review and meta-analysis. J Am Coll Cardiol 58:2241–2247. https://doi.org/10.1016/j.jacc.2011.08.025
2. Hoang TT, Goldmuntz E, Roberts AE et al (2018) The congenital heart disease genetic network study: cohort description. PLoS ONE 13:e0191319. https://doi.org/10.1371/journal.pone.0191319
3. Metcalf MK, Rychik J (2020) Outcomes in hypoplastic left heart syndrome. Pediatr Clin North Am 67:945–962. https://doi.org/10.1016/j.pcl.2020.06.008
4. Kritzmire SM, Cossu AE (2022) Hypoplastic Left Heart Syndrome. In: StatPearls. StatPearls Publishing, Treasure Island (FL).
5. Bejjani AT, Wary N, Gu M (2021) Hypoplastic left heart syndrome (HLHS): molecular pathogenesis and emerging drug targets for cardiac repair and regeneration. Expert Opin Ther Targets 25:621–632. https://doi.org/10.1080/14728222.2021.1978069
6. Danford DA, Cronican P (1992) Hypoplastic left heart syndrome: Progression of left ventricular dilation and dysfunction to left ventricular hypoplasia in utero. Am Heart J 123:1712–1713. https://doi.org/10.1016/0002-8703(92)90834-I
7. Simpson JM, Sharland GK (1997) Natural history and outcome of aortic stenosis diagnosed prenatally. Heart 77:205–210
8. Apitz C, Webb GD, Redington AN (2009) Tetralogy of fallot. Lancet 374:1462–1471. https://doi.org/10.1016/S0140-6736(09)60657-7
9. Fisher DJ, Heymann MA, Rudolph AM (1982) Regional myocardial blood flow and oxygen delivery in fetal, newborn, and adult sheep. Am J Physiol 243:H729-731. https://doi.org/10.1152/ajpheart.1982.243.5.H729
10. Taverne YJHJ, Sadeghi A, Bartelds B et al (2021) Right ventricular phenotype, function, and failure: a journey from evolution to clinics. Heart Fail Rev 26:1447–1466. https://doi.org/10.1007/s10741-020-09982-4

11. Razeghi P, Young ME, Alcorn JL et al (2001) Metabolic gene expression in fetal and failing human heart. Circulation 104:2923–2931. https://doi.org/10.1161/hc4901.100526
12. Asp J, Synnergren J, Jonsson M et al (2012) Comparison of human cardiac gene expression profiles in paired samples of right atrium and left ventricle collected in vivo. Physiol Genomics 44:89–98. https://doi.org/10.1152/physiolgenomics.00137.2011
13. Gorr MW, Sriram K, Chinn AM et al (2020) Transcriptomic profiles reveal differences between the right and left ventricle in normoxia and hypoxia. Physiol Rep 8:e14344. https://doi.org/10.14814/phy2.14344
14. Lei I, Huang W, Ward PA et al (2021) Differential inflammatory responses of the native left and right ventricle associated with donor heart preservation. Physiol Rep 9:e15004. https://doi.org/10.14814/phy2.15004
15. Mercuro G, Bassareo PP, Mariucci E et al (2014) Sex differences in congenital heart defects and genetically induced arrhythmias. J Cardiovasc Med (Hagerstown) 15:855–863. https://doi.org/10.2459/JCM.0b013e32835ec828
16. Storch TG, Mannick EE (1992) Epidemiology of congenital heart disease in Louisiana: an association between race and sex and the prevalence of specific cardiac malformations. Teratology 46:271–276. https://doi.org/10.1002/tera.1420460311
17. Karamlou T, Diggs BS, Ungerleider RM, Welke KF (2010) Evolution of treatment options and outcomes for hypoplastic left heart syndrome over an 18-year period. J Thorac Cardiovasc Surg 139:119–126. https://doi.org/10.1016/j.jtcvs.2009.04.061
18. Ohye RG, Sleeper LA, Mahony L et al (2010) Comparison of shunt types in the Norwood procedure for single-ventricle lesions. N Engl J Med 362:1980–1992. https://doi.org/10.1056/NEJMoa0912461
19. Surerus E, Huggon IC, Allan LD (2003) Turner's syndrome in fetal life. Ultrasound Obstet Gynecol 22:264–267. https://doi.org/10.1002/uog.151
20. Sharma V, Goessling LS, Brar AK et al (2021) Coxsackievirus B3 infection early in pregnancy induces congenital heart defects through suppression of fetal cardiomyocyte proliferation. J Am Heart Assoc 10:e017995. https://doi.org/10.1161/JAHA.120.017995
21. Breuer K, Foroushani AK, Laird MR et al (2013) InnateDB: systems biology of innate immunity and beyond–recent updates and continuing curation. Nucleic Acids Res 41:D1228-1233. https://doi.org/10.1093/nar/gks1147
22. Huang SSY, Makhlouf M, AbouMoussa EH et al (2020) Differential regulation of the immune system in a brain-liver-fats organ network during short-term fasting. Mol Metab 40:101038. https://doi.org/10.1016/j.molmet.2020.101038
23. Yu G (2020) Gene ontology semantic similarity analysis using GOSemSim. Methods Mol Biol 2117:207–215. https://doi.org/10.1007/978-1-0716-0301-7_11
24. Langfelder P, Zhang B, Horvath S (2008) Defining clusters from a hierarchical cluster tree: the dynamic tree cut package for R. Bioinformatics 24:719–720. https://doi.org/10.1093/bioinformatics/btm563
25. Supek F, Bošnjak M, Škunca N, Šmuc T (2011) REVIGO summarizes and visualizes long lists of gene ontology terms. PLoS ONE 6:e21800. https://doi.org/10.1371/journal.pone.0021800
26. Febbo PG, Mulligan MG, Slonina DA et al (2007) Literature Lab: a method of automated literature interrogation to infer biology from microarray analysis. BMC Genomics 8:461. https://doi.org/10.1186/1471-2164-8-461
27. Chhangawala S, Rudy G, Mason CE, Rosenfeld JA (2015) The impact of read length on quantification of differentially expressed genes and splice junction detection. Genome Biol 16:131. https://doi.org/10.1186/s13059-015-0697-y
28. Ce M et al (2018) Identification of optimal reference genes for transcriptomic analyses in normal and diseased human heart. Cardiovasc Res. https://doi.org/10.1093/cvr/cvx182
29. Ontsouka E, Lüthi M, Zaugg J et al (2021) Establishment and validation of an approach allowing unequivocal fetal sex determination based on placental sex-specific genes. Placenta 112:132–134. https://doi.org/10.1016/j.placenta.2021.07.295
30. Lefèvre N, Corazza F, Duchateau J et al (2012) Sex differences in inflammatory cytokines and CD99 expression following in vitro lipopolysaccharide stimulation. Shock 38:37–42. https://doi.org/10.1097/SHK.0b013e3182571e46
31. Ma W et al (2022) Sex-biased and parental allele-specific gene regulation by KDM6A. Biol Sex Differences. https://doi.org/10.1186/s13293-022-00452-0
32. Bamforth SD, Bragança J, Farthing CR et al (2004) Cited2 controls left-right patterning and heart development through a Nodal-Pitx2c pathway. Nat Genet 36:1189–1196. https://doi.org/10.1038/ng1446
33. Pierpont ME, Brueckner M, Chung WK et al (2018) Genetic basis for congenital heart disease: revisited: a scientific statement from the american heart association. Circulation 138:e653–e711. https://doi.org/10.1161/CIR.0000000000000606
34. Mohapatra B, Casey B, Li H et al (2009) Identification and functional characterization of NODAL rare variants in heterotaxy and isolated cardiovascular malformations. Hum Mol Genet 18:861–871. https://doi.org/10.1093/hmg/ddn411
35. Franco D, Sedmera D, Lozano-Velasco E (2017) Multiple roles of Pitx2 in cardiac development and disease. J Cardiovasc Dev Dis 4:16. https://doi.org/10.3390/jcdd4040016
36. Patel K, Isaac A, Cooke J (1999) Nodal signalling and the roles of the transcription factors SnR and Pitx2 in vertebrate left-right asymmetry. Curr Biol 9:609–612. https://doi.org/10.1016/s0960-9822(99)80267-x
37. Desgrange A, Le Garrec J-F, Bernheim S et al (2020) Transient nodal signaling in left precursors coordinates opposed asymmetries shaping the heart loop. Dev Cell 55:413-431.e6. https://doi.org/10.1016/j.devcel.2020.10.008
38. Yoshiba S, Hamada H (2014) Roles of cilia, fluid flow, and Ca2+ signaling in breaking of left–right symmetry. Trends Genet 30:10–17. https://doi.org/10.1016/j.tig.2013.09.001
39. Swirski FK, Nahrendorf M (2018) Cardioimmunology: the immune system in cardiac homeostasis and disease. Nat Rev Immunol 18:733–744. https://doi.org/10.1038/s41577-018-0065-8
40. Isensee J, Witt H, Pregla R et al (2008) Sexually dimorphic gene expression in the heart of mice and men. J Mol Med (Berl) 86:61–74. https://doi.org/10.1007/s00109-007-0240-z
41. Spolski R (2018) Biology and regulation of IL-2: from molecular mechanisms to human therapy. Nat Rev Immunol. https://doi.org/10.1038/s41577-018-0046-y
42. Healy AM, Izmailova E, Fitzgerald M et al (2006) PKC-theta-deficient mice are protected from Th1-dependent antigen-induced arthritis. J Immunol 177:1886–1893. https://doi.org/10.4049/jimmunol.177.3.1886
43. Tan S-L, Zhao J, Bi C et al (2006) Resistance to experimental autoimmune encephalomyelitis and impaired IL-17 production in protein kinase C theta-deficient mice. J Immunol 176:2872–2879. https://doi.org/10.4049/jimmunol.176.5.2872
44. Sen S, Wang F, Zhang J et al (2018) SRC1 promotes Th17 differentiation by overriding Foxp3 suppression to stimulate RORγt activity in a PKC-θ-dependent manner. Proc Natl Acad Sci U S A 115:E458–E467. https://doi.org/10.1073/pnas.1717789115
45. Xo Y, Ad P et al (2007) STAT3 regulates cytokine-mediated generation of inflammatory helper T cells. J Biol Chem. https://doi.org/10.1074/jbc.C600321200

46. Krishnan A, Samtani R, Dhanantwari P et al (2014) A detailed comparison of mouse and human cardiac development. Pediatr Res 76:500–507. https://doi.org/10.1038/pr.2014.128
47. Lj M, Kl J, Tm S et al (2014) Amniotic fluid RNA gene expression profiling provides insights into the phenotype of turner syndrome. Human Genet. https://doi.org/10.1007/s00439-014-1448-y
48. Wang H, Zhu H, Zhu W et al (2020) Bioinformatic analysis identifies potential key genes in the pathogenesis of turner syndrome. Front Endocrinol (Lausanne) 11:104. https://doi.org/10.3389/fendo.2020.00104
49. Xu Z (2010) Plasminogen activator inhibitor-1 (PAI-1) is cardioprotective in mice by maintaining microvascular integrity and cardiac architecture. Blood. https://doi.org/10.1182/blood-2009-09-244962
50. Flevaris P, Khan SS, Eren M et al (2017) Plasminogen activator inhibitor type I controls cardiomyocyte transforming growth Factor-β and cardiac fibrosis. Circulation 136:664–679. https://doi.org/10.1161/CIRCULATIONAHA.117.028145
51. Ghosh AK, Kalousdian AA, Shang M et al (2023) Cardiomyocyte PAI-1 influences the cardiac transcriptome and limits the extent of cardiac fibrosis in response to left ventricular pressure overload. Cell Signal 104:110555. https://doi.org/10.1016/j.cellsig.2022.110555
52. Bhattacharya S et al (2018) ImmPort, toward repurposing of open access immunological assay data for translational and clinical research. Sci Data. https://doi.org/10.1038/sdata.2018.15
53. Cm P et al (2017) The psoriasis-associated IL-17A induces and cooperates with IL-36 cytokines to control keratinocyte differentiation and function. Sci Rep. https://doi.org/10.1038/s41598-017-15892-7
54. Rani L et al (2022) IL-3 regulates the differentiation of pathogenic Th17 cells. European J Immunol. https://doi.org/10.1002/eji.202149674
55. Koop BF, Rowen L, Wang K et al (1994) The human T-cell receptor TCRAC/TCRDC (C alpha/C delta) region: organization, sequence, and evolution of 97.6 kb of DNA. Genomics 19:478–493. https://doi.org/10.1006/geno.1994.1097
56. Borrego F (2013) The CD300 molecules: an emerging family of regulators of the immune system. Blood 121:1951–1960. https://doi.org/10.1182/blood-2012-09-435057
57. Haga K, Fujimoto A, Takai-Todaka R et al (2016) Functional receptor molecules CD300lf and CD300ld within the CD300 family enable murine noroviruses to infect cells. Proc Natl Acad Sci U S A 113:E6248–E6255. https://doi.org/10.1073/pnas.1605575113
58. Schubert M et al (2018) Perturbation-response genes reveal signaling footprints in cancer gene expression. Nat Commun. https://doi.org/10.1038/s41467-017-02391-6
59. Cui Y, Zheng Y, Liu X et al (2019) Single-cell transcriptome analysis maps the developmental track of the human heart. Cell Rep 26:1934-1950.e5. https://doi.org/10.1016/j.celrep.2019.01.079
60. Schlesinger J, Schueler M, Grunert M et al (2011) The cardiac transcription network modulated by Gata4, Mef2a, Nkx2.5, Srf, histone modifications, and microRNAs. PLoS Genet 7:e1001313. https://doi.org/10.1371/journal.pgen.1001313
61. Lary JM, Paulozzi LJ (2001) Sex differences in the prevalence of human birth defects: a population-based study. Teratology 64:237–251. https://doi.org/10.1002/tera.1070
62. Smith KLM, Swiderska A, Lock MC et al (2022) Chronic developmental hypoxia alters mitochondrial oxidative capacity and reactive oxygen species production in the fetal rat heart in a sex-dependent manner. J Pineal Res 73:e12821. https://doi.org/10.1111/jpi.12821
63. Lp T (2020) Sex differences and the effects of intrauterine hypoxia on growth and in vivo heart function of fetal guinea pigs. American J Physiol Regulat, Integr Compar Physiol. https://doi.org/10.1152/ajpregu.00249.2019
64. Gabriel GC, Lo CW (2020) Left–right patterning in congenital heart disease beyond heterotaxy. Am J Med Genet C Semin Med Genet 184:90. https://doi.org/10.1002/ajmg.c.31768
65. Roessler E, Ouspenskaia MV, Karkera JD et al (2008) Reduced NODAL signaling strength via mutation of several pathway members including FOXH1 is linked to human heart defects and holoprosencephaly. American J Human Genet 83:18–29. https://doi.org/10.1016/j.ajhg.2008.05.012
66. Bg B (2013) Signaling and transcriptional networks in heart development and regeneration. Cold Spring Harbor Perspect Biol. https://doi.org/10.1101/cshperspect.a008292
67. Leid J, Carrelha J, Boukarabila H et al (2016) Primitive embryonic macrophages are required for coronary development and maturation. Circ Res 118:1498–1511. https://doi.org/10.1161/CIRCRESAHA.115.308270
68. Patterson AJ, Zhang L (2010) Hypoxia and fetal heart development. Curr Mol Med 10:653–666. https://doi.org/10.2174/156652410792630643
69. Mercurio L, Failla CM, Capriotti L et al (2020) Interleukin (IL)-17/IL-36 axis participates to the crosstalk between endothelial cells and keratinocytes during inflammatory skin responses. PLoS ONE 15:e0222969. https://doi.org/10.1371/journal.pone.0222969
70. Barin JG, Baldeviano GC, Talor MV et al (2012) Macrophages participate in IL-17-mediated inflammation. Eur J Immunol 42:726–736. https://doi.org/10.1002/eji.201141737
71. Germán B, Wei R, Hener P et al (2019) Disrupting the IL-36 and IL-23/IL-17 loop underlies the efficacy of calcipotriol and corticosteroid therapy for psoriasis. JCI Insight 4:e123390. https://doi.org/10.1172/jci.insight.123390
72. Weng Y-J, Hsieh DJ-Y, Kuo W-W et al (2010) E4BP4 is a cardiac survival factor and essential for embryonic heart development. Mol Cell Biochem 340:187–194. https://doi.org/10.1007/s11010-010-0417-6
73. Laurence A, Tato CM, Davidson TS et al (2007) Interleukin-2 signaling via STAT5 constrains T helper 17 cell generation. Immunity 26:371–381. https://doi.org/10.1016/j.immuni.2007.02.009
74. Xie H, Sadim MS, Sun Z (2005) RORgammat recruits steroid receptor coactivators to ensure thymocyte survival. J Immunol 175:3800–3809. https://doi.org/10.4049/jimmunol.175.6.3800
75. Haas JD, Ravens S, Düber S et al (2012) Development of interleukin-17-producing γδ T cells is restricted to a functional embryonic wave. Immunity 37:48–59. https://doi.org/10.1016/j.immuni.2012.06.003
76. Agerholm R, Rizk J, Viñals MT, Bekiaris V (2019) STAT3 but not STAT4 is critical for γδT17 cell responses and skin inflammation. EMBO Rep 20:e48647. https://doi.org/10.15252/embr.201948647
77. Zuberbuehler MK, Parker ME, Wheaton JD et al (2019) The transcription factor c-Maf is essential for the commitment of IL-17-producing γδ T cells. Nat Immunol 20:73–85. https://doi.org/10.1038/s41590-018-0274-0
78. Miao Y, Tian L, Martin M et al (2020) Intrinsic endocardial defects contribute to hypoplastic left heart syndrome. Cell Stem Cell 27:574-589.e8. https://doi.org/10.1016/j.stem.2020.07.015
79. Bach LA (2015) Endothelial cells and the IGF system. J Mol Endocrinol 54:R1-13. https://doi.org/10.1530/JME-14-0215
80. Shigeta A, Huang V, Zuo J et al (2019) Endocardially-derived macrophages are essential for valvular remodeling. Dev Cell 48:617-630.e3. https://doi.org/10.1016/j.devcel.2019.01.021
81. Rahman MdS, Jun H (2022) The adipose tissue macrophages central to adaptive thermoregulation. Front Immunol 13:884126. https://doi.org/10.3389/fimmu.2022.884126

82. Cunningham TJ, Duester G (2015) Mechanisms of retinoic acid signalling and its roles in organ and limb development. Nat Rev Mol Cell Biol 16:110–123. https://doi.org/10.1038/nrm3932
83. Das BC, Thapa P, Karki R et al (2014) Retinoic acid signaling pathways in development and diseases. Bioorg Med Chem 22:673–683. https://doi.org/10.1016/j.bmc.2013.11.025
84. Vieux-Rochas M, Coen L, Sato T et al (2007) Molecular dynamics of retinoic acid-induced craniofacial malformations: implications for the origin of gnathostome jaws. PLoS ONE 2:e510. https://doi.org/10.1371/journal.pone.0000510
85. Uribe RA, Hong SS, Bronner ME (2018) Retinoic acid temporally orchestrates colonization of the gut by vagal neural crest cells. Dev Biol 433:17–32. https://doi.org/10.1016/j.ydbio.2017.10.021
86. Williams AL, Bohnsack BL (2019) What's retinoic acid got to do with it? Retinoic acid regulation of the neural crest in craniofacial and ocular development. Genesis 57:7. https://doi.org/10.1002/dvg.23308
87. Trainor PA (2005) Specification of neural crest cell formation and migration in mouse embryos. Semin Cell Dev Biol 16:683–693. https://doi.org/10.1016/j.semcdb.2005.06.007
88. Thorogood P, Smith L, Nicol A et al (1982) Effects of vitamin A on the behaviour of migratory neural crest cells in vitro. J Cell Sci 57:331–350. https://doi.org/10.1242/jcs.57.1.331
89. Conway SJ, Bundy J, Chen J et al (2000) Decreased neural crest stem cell expansion is responsible for the conotruncal heart defects within the Splotch (Sp2H)/Pax3 mouse mutant. Cardiovasc Res 47:314–328. https://doi.org/10.1016/S0008-6363(00)00098-5
90. Wang C, Zhang R, Wei X et al (2020) Metalloimmunology: the metal ion-controlled immunity. Adv Immunol 145:187–241. https://doi.org/10.1016/bs.ai.2019.11.007
91. Pervolaraki E, Dachtler J, Anderson RA, Holden AV (2018) The developmental transcriptome of the human heart. Sci Rep 8:15362. https://doi.org/10.1038/s41598-018-33837-6
92. Suryawanshi H, Clancy R, Morozov P et al (2020) Cell atlas of the foetal human heart and implications for autoimmune-mediated congenital heart block. Cardiovasc Res 116:1446–1457. https://doi.org/10.1093/cvr/cvz257